Optics Letters

Loss tailoring of high-power broad-area diode lasers

LIJIE WANG,[1] CUNZHU TONG,[1,*] SHILI SHU,[1] SICONG TIAN,[1] FANGYUAN SUN,[1,2] YUFEI ZHAO,[1,2] HUANYU LU,[1,2] XIN ZHANG,[1] GUANYU HOU,[1,2] AND LIJUN WANG[1]

[1]State Key Laboratory of Luminescence and Applications, Changchun Institute of Optics, Fine Mechanics and Physics (CIOMP), Chinese Academy of Sciences, Changchun 130033, China
[2]Center of Materials Science and Optoelectronics Engineering, the University of Chinese Academy of Sciences, Beijing100049, China
*Corresponding author: tongcz@ciomp.ac.cn

Received 15 May 2019; revised 19 June 2019; accepted 19 June 2019; posted 19 June 2019 (Doc. ID 367578); published 12 July 2019

Broad-area diode lasers (BALs) with high power are highly desirable for a variety of applications. However, such lasers suffer from strongly deteriorated beam quality due to multimode behavior in the lateral direction. In this Letter, we present an approach to flexibly tailor the optical loss of different-order lateral modes by etching micro-holes on the laser mesa with controlled position and numbers. Through arranging the micro-holes at the peak positions of high-order lateral modes with an increasing number from the mesa center to both edges, high-order modes are suppressed due to a larger propagation loss than the fundamental mode. As a result of enhanced mode discrimination, we demonstrate that this technique provides a greatly improved beam quality and about two times higher brightness for 100 μm wide BAL, while maintaining high power and slope efficiency output.

https://doi.org/10.1364/OL.44.003562

Diode lasers have been increasingly attractive in recent years due to the advantages of high efficiency, electrical pumping, compact size, broad wavelength range, and long lifetime. With the development of diode laser technology and beam combining technology, the power and brightness of diode lasers have been appreciably improved, leading to a growing market in pumping, material processing, display, and medical applications [1–3]. Based on advanced combining technologies such as spectral beam combining, kW-class direct-diode lasers have been developed with a beam quality similar to or better than the value of commercial CO_2 and solid lasers [4]. However, the brightness of all beam combining systems is ultimately limited by the beam quality of their single emitters, which still has a large gap to the performance of fiber lasers recently reported [5–7]. Therefore, improving the beam quality of a single emitter while sustaining high power and efficiency is a key challenge for high brightness diode laser sources.

Broad-area diode lasers (BALs) are the most important type of commercial diode lasers due to their high output power and simple manufacturing process. However, the low mode discrimination of the BAL wide emitter size easily leads to a large number of lateral modes [8]. The excitation of higher-order lateral modes is mainly produced by the following physical mechanisms: a thermal lens induced by self-heating, lateral carrier accumulation at the stripe edges, etched trench-induced index guiding, vertical epitaxial layer design, filamentation, mechanical strain, and so on [9–11]. For specific diode laser chips, the first two factors play the most critical role, leading to a rising number of lateral modes at high-power operation. Under a high injection current, the enhanced lateral temperature gradient leads to an increase of the lateral index step and waveguiding, supporting higher-order modes. Simultaneously, the current crowding near the stripe edges provides more gain to high-order modes. As a result, the BALs usually suffer from a quickly widening lateral far-field (FF) with increasing current, a so-called FF blooming effect. This results in poor lateral beam quality and reduced brightness, limiting their direct applications.

For reducing the allowed number of lateral modes and improving the beam quality, many approaches are proposed. Optimized epitaxial design, chip geometry, and packaging are beneficial to suppress the thermal lensing effect due to less self-heat generating and junction temperature rising [12]. Complex pedestal heatsink is also utilized to reduce the lateral temperature gradient by inverse thermal lens effects [13]. Trimming the emitter width could cut the number of modes, but with the price of a cut in the output power [14]. A uniform gain profile across the contact is favorable for increasing optical field stabilization through utilizing the gain-tailored structure or current path structure such as the phase-locked array, multi-stripe gain structure, or current modulation structure [15–17]. In addition, the suppression of lateral carrier accumulation by deep proton implantation can effectively improve the beam quality [18]. Another effective way is introducing mode filters to produce extra losses for high-order modes such as the tapered laser, phase structure, external cavity configure, titled waveguide, microstructure, and inhomogeneous waveguide [19–26]. All these methods have improved the brightness of diode lasers. However, most of them could not achieve significant improvements in lateral beam quality without obviously

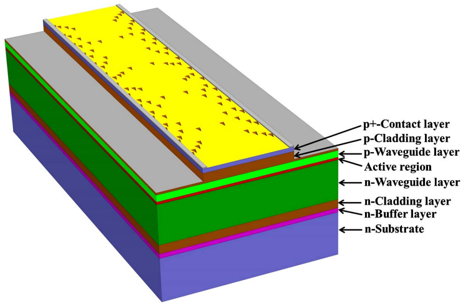

Fig. 1. Schematic diagram of the loss tailoring BAL.

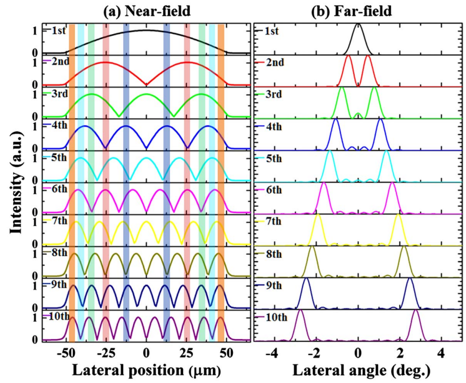

Fig. 2. Calculated (a) near-field and (b) far–field profiles of the lateral mode with different mode orders.

sacrificing laser efficiency and power. Furthermore, some methods are technologically complicated and, thus, limited in their applicability.

Here we describe a method to introduce different optical losses for each lateral mode, which enables extracting the desired mode to operate. In order to improve the beam quality of BALs, distributed micro-holes are etched at the optical peak positions of high-order modes with variant numbers, providing additional losses for higher-order modes while minimizing the loss of the fundamental mode. In this Letter, the details of the laser structures and fabrication process are first presented. Then the power-current characteristics and spatial beam properties of the structured BALs are described and compared with standard BALs from the same wafer. We show experimentally that such enhanced mode selectivity achieves an obvious improvement in beam quality without reducing the slope efficiency and output power.

The device structure of the loss tailoring BAL is schematically shown in Fig. 1. The laser heterostructure was grown on an n-type GaAs substrate by a metal-organic chemical vapor deposition system, which makes use of an asymmetric large optical cavity structure. The gain medium is two InGaAs/GaAsP quantum wells and is sandwiched between a 3.0 μm $Al_{0.15}Ga_{0.85}As$ n-waveguide and 0.4 μm $Al_{0.2}Ga_{0.8}As$ p-waveguide. The emission wavelength is designed to be about 965 nm. The cladding layers are chosen to be 0.5 μm $Al_{0.35}Ga_{0.65}As$ and 0.8 μm $Al_{0.5}Ga_{0.5}As$, respectively, in the n- and p-doped sides. The doping profiles and all interfaces are graded to reduce the series resistance while maintaining a low internal loss.

In this Letter, the experiment was conducted on the BALs with a stripe width of 100 μm, which operated in multi-lateral modes. The lateral optical modes have different spatial intensity distributions and FF patterns. For a simplified discussion, the approximate near-field and FF profiles of individual lateral modes are shown in Fig. 2. Except for the first mode (fundamental mode), higher-order modes exhibit a FF profile consisting of two main lobes with some small lobes. The separation angle of twin main lobes rises linearly at a rate of about 0.59° per mode order. The higher the lateral mode order, the wider is the FF width. When the injection current increases, a strong heat-induced index gradient and current crowding near the contact edges will support more high-order modes due to an equalized mode gain. Simultaneously, the near-field width of each mode would reduce, leading to a wider FF. Therefore, the increased number of lateral modes and the widening FF of each mode result in a rapid increase in the optical field and a deteriorated beam quality [10,13].

For traditional BALs under continuous-wave (CW) operation, the lateral modes are nearly competitive with each other due to a low gain difference and, consequently, weak mode discrimination [16,25]. The etched micro-holes down to the waveguide region could selectively induce light loss due to scattering and absorption. In order to extract the desired mode, many rows of micro-holes can be etched on the laser mesa to provide preferential losses to undesired modes. The shape, depth, position, and number of holes are carefully controlled to achieve a better balance between enhanced mode discrimination and a minimal change in threshold and slope efficiency.

In this Letter, we choose isosceles triangle holes with a width of 5 μm and a height of 20 μm. To suppress high-order lateral modes, these micro-holes are arranged along the optical peak positions of high-order modes, while the number of holes along the propagation direction increases from the middle region toward the stripe edge. The central region of the stripe is free of holes, corresponding to the intensity maximum of the fundamental mode. Due to their significant optical intensities in the structured region and a larger number of holes near the edge region, high-order laser modes suffer from a much higher propagation loss than the central fundamental mode. Such enhanced mode discrimination enables reducing the permissible number of lateral modes. As our ultimate aim is to develop laser bars with a high fill factor for spectrum combining, each emitter operates at a relatively low power level. Referring to the optical field of each mode at low currents, we etched 10 rows of micro-holes symmetrically in the lateral direction which, respectively, are located at the intensity maxima of the fourth, second, third, and fifth mode and the device edges. The location of the hole rows can be seen in the transparent columns in Figs. 2(a) and 1. The micro-holes are distributed along the entire cavity with a scaling number of 4, 8, 10, 12, and 14 from the mesa center to both sides.

After the material growth, the devices were processed following a standard BAL fabrication procedure. First, 100 μm wide mesa, air-hole patterns and 30 μm wide trenches were defined by lithography and inductively coupled plasma etching, respectively. The etching depth of the micro-holes was about 1.2 μm, slightly touching the waveguide region. In this case, the etched holes moderately overlapped with the optical field of the guided transverse mode in order to avoid significant optical loss. Then a 300 nm SiO_2 electrical insulating layer was deposited, and the

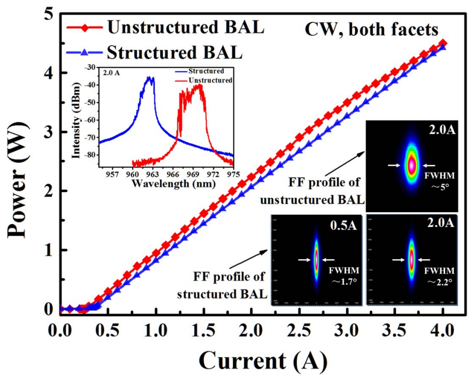

Fig. 3. Optical power versus the injection current of the lasers with and without micro-holes under continuous operation. The top-left inset shows the measured spectra, and the bottom-right inset shows the measured far-field patterns for both devices.

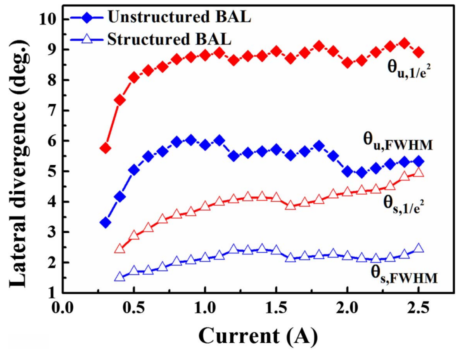

Fig. 4. Measured lateral divergence angle as a function of the injected current, triangle (structured laser), and diamond (unstructured laser).

contact window was opened by reactive ion etching. After that, p-side metal contact deposition, substrate thinning, polishing, and n-metallization were performed. Finally, single emitters with a cavity length of 1.5 mm were cleaved and bonded p-side down on C-mount copper heatsinks using an indium solder without facet coating and passivation. Conventional BALs without micro-hole patterns were also fabricated from the same wafer for comparison.

Figure 3 shows the power-current characteristics of the structured and unstructured BALs under CW operation at room temperature. As can be seen, the laser without micro-holes has a threshold current of 0.3 A and a slope efficiency of about 1.2 W/A. The threshold current of the laser with micro-holes was slightly increased to 0.35 A. However, the structured laser has nearly the same slope efficiency of 1.2 W/A and total power of 4.4 W at 4 A current. As the micro-holes only induce small extra losses to suppress high-order modes, the result is a small reduction in the slope efficiency [25]. Furthermore, the micro-hole scattering and reduced mode competition can transfer the strong emission from the stripe edges to generate a more uniform near field [27]. The improved overlap between carrier and optical distributions is able to increase power conversion efficiency. Therefore, a similar slope efficiency is obtained for both lasers. The voltage performances for both devices are almost the same. The lasing spectra of these two kinds of devices at 2.0 A current are shown in the top-left inset of Fig. 3. The center wavelength for the structured BAL is 962.5 nm, about 7 nm shifting from the standard BAL due to variations in the epitaxy. However, the structured BAL shows a narrower spectral width due to the reduced number of guided lateral modes.

The measured FF patterns of both lasers are shown in the bottom-right inset of Fig. 3. Both lasers show similar beam profiles in the vertical direction with a FF angle of about 14° for the full width at half-maximum (FWHM), which are almost independent on the current. In the lateral direction, the structured laser shows an improved FF behavior, which exhibits a much narrower lateral FF than the unstructured BAL, even under high injection conditions.

Figure 4 depicts the dependence of lateral divergence angle as a function of injected current for the structured and unstructured lasers. The largest measurement current is limited to 2.5 A due to the saturation of our beam profiler. For the unstructured laser, the lateral divergence angle θ_u is 3.3° (FWHM) and 5.8° ($1/e^2$) at the threshold current, which rapidly broadens to 5.5° (FWHM) and 8.3° ($1/e^2$) at 0.6 A current related to the additional oscillation of high-order modes. With the further increase of the injection current, the lateral divergence slightly increases to about 9.1° for the $1/e^2$ content at 2.5 A. On the other hand, the introduction of micro-holes results not only in a reduction of the divergence angle, but also in a more stable FF. The lateral divergence angle θ_s of the structured laser is only 1.5° (FWHM) and 2.4° ($1/e^2$) at 0.4 A current, and slightly increases to 2.4° (FWHM) and 4.9° ($1/e^2$) at 2.5 A. It is important to note that the increasing rate has some kinks, which may result from the mode switching of high-order modes. As can be seen in Fig. 4, about 50% reduction of the lateral divergence angle is achieved as a result of tailoring the optical mode loss. This demonstrates that the micro-hole structure is beneficial for yielding reduced and stabilized FF divergence angles.

The lateral beam quality of the fabricated lasers was measured by a commercial beam propagation analyzer M2MS-BP209 according to the ISO11146 standard. In Fig. 5, the lateral beam quality is plotted as a function of the injection current for both kinds of lasers. As can be observed, a clear improvement in the lateral beam quality is achieved by loss tailoring. For the conventional BAL, the lateral beam quality M^2 degrades from 4.33 at 0.6 A to 15.11 at 4.0 A current due to a

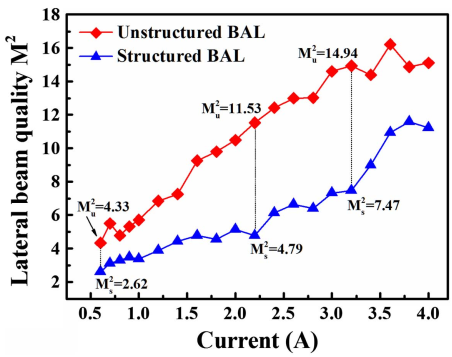

Fig. 5. Lateral beam quality of the structured and unstructured BALs at different currents under CW operation.

fast increasing number of lasing modes. The laser beam quality M^2 factor has been significantly reduced for the structured laser. As a result of the suppression of high-order modes, the M^2 value reduces to 2.62 at 0.6 A current and shows a much lower increasing rate with the current until 3.2 A, at which the beam quality is improved from 14.94 to 7.47 by an improving factor of >50%. In particular, at 2.2 A, the M^2 value is reduced from 11.53 to 4.79 by a factor of as high as 58%. The corresponding lateral brightness increases from 0.7 W/mm × mrad to 1.56 W/mm × mrad, improved by a factor of 2.2. However, when the current is beyond 3.2 A, the M^2 value of the structured BAL begins to suffer from a rapid increase, which increases to 11 at 4.0 A current. This may result from the serious self-heat of the devices limited by the packaging condition. In our experiment, the laser chip without thick Au contact deposition is soft soldered on a copper heatsink with an un-polishing surface, which is not able to transfer heat effectively under large currents in CW operation. The enhancement of thermal-induced guiding may support more modes to oscillate and lead to a significant near-field reduction of each mode. This will result in offsets from the optical peak locations of some high-order modes to the structured region, weakening the mode-discriminating effect.

From the results shown above, the BAL with loss tailoring structures is advantageous for improving the laser brightness, which is promising for beam combining systems. Furthermore, the beam quality of output beam can be enhanced further by improving the packaging technology and optimizing the parameters of micro-holes such as enlarging the number of micro-holes at the stripe edge and increasing the etching depth. If the placement of micro-holes is re-designed to match the realistic near-field profile of the BAL under a high injection current, the mode selection would remain effective at even higher power operation, thus increasing the brightness. It also would be of interest to apply the approach to BAL with a narrower stripe width, or to collaborate with other methods for reducing thermal lens effect and carrier accumulation at the device edges.

In summary, we have presented an approach to suppress high-order lateral modes by the help of specifically etched micro-holes, which provide extra propagation loss for high-order modes. As a result of selectively loss tailoring, a reduced number of active lateral modes allows for an effective improvement of the beam quality without obvious power degradation, increasing the laser brightness. The lateral FF divergence of a 100 μm wide BAL narrows by about 50% in the whole measurement range. In addition, the structured BAL delivered an obvious improvement in the beam quality compared with traditional BALs, whose peak brightness is increased by more than a factor of 2. By further optimization in the micro-hole parameters and packaging processes, higher brightness can be expected. This technique gives a way to develop high brightness diode laser without increasing the fabrication complexity and cost.

Funding. National Natural Science Foundation of China (NSFC) (61474119, 61761136009, 61774153, 61774156); Chinese Academy of Sciences (CAS) (181722KYSB20160005); Natural Science Foundation of Jilin Province (20180519024JH, 20190302053GX); China Scholarship Council (CSC) (201704910183).

REFERENCES

1. C. X. Yu, O. Shatrovoy, T. Y. Fan, and T. F. Taunay, Opt. Lett. **41**, 5202 (2016).
2. U. Witte, F. Schneider, M. Traub, D. Hoffmann, S. Droves, T. Brand, and A. Unger, Opt. Express **24**, 22917 (2016).
3. A. Pietrzak, M. Zorn, R. Huelsewede, J. Meusel, and J. Sebastian, Proc. SPIE **10900**, 109000K (2019).
4. R. K. Huang, B. Chann, J. Burgess, B. Lochman, W. Zhou, M. Cruz, R. Cook, D. Dugmore, J. Shattuck, and P. Tayebati, Proc. SPIE **9730**, 97300C (2016).
5. S. Hengesbach, N. Krauch, C. Holly, M. Traub, U. Witte, and D. Hoffmann, Opt. Lett. **38**, 3154 (2013).
6. H. C. Meng, T. Y. Sun, H. Tan, J. H. Yu, W. C. Du, F. Tian, J. M. Li, S. X. Gao, X. J. Wang, and D. Y. Wu, Opt. Express **23**, 21819 (2015).
7. H. B. Zhu, X. C. Lin, Y. W. Zhang, J. W. Zhang, B. Wang, J. L. Zhang, L. Qin, Y. Q. Ning, and H. Wu, Opt. Express **26**, 24723 (2018).
8. S. Gross, D. W. Coutts, M. Dubinskiy, and M. J. Withford, Opt. Lett. **44**, 831 (2019).
9. P. Crump, S. Böldicke, C. M. Schultz, H. Ekhteraei, H. Wenzel, and G. Erbert, Semicond. Sci. Technol. **27**, 045001 (2012).
10. M. Winterfeldt, P. Crump, H. Wenzel, G. Erbert, and G. Tränkle, J. Appl. Phys. **116**, 063103 (2014).
11. M. Winterfeldt, J. Rieprich, S. Knigge, A. Maaßdorf, M. Hempel, R. Kernke, J. W. Tomm, G. Erbert, and P. Crump, Proc. SPIE **9733**, 97330O (2016).
12. J. Rieprich, M. Winterfeldt, R. Kernke, J. W. Tomm, and P. Crump, J. Appl. Phys. **123**, 125703 (2018).
13. J. Piprek, IEEE Photonics Technol. Lett. **25**, 958 (2013).
14. Y. Lia, W. C. Du, K. Zhou, J. J. Kang, S. X. Gao, D. Y. Wu, Y. Hu, L. Zhang, H. Tan, and C. Tang, Proc. SPIE **11023**, 110234H (2019).
15. W. Zhou, S. Slivken, and M. Razeghi, Appl. Phys. Lett. **112**, 181106 (2018).
16. A. Maląg, G. Sobczak, E. Dąbrowska, and M. Teodorczyk, Proc. SPIE **10974**, 1097404 (2018).
17. T. Wang, C. Z. Tong, L. J. Wang, Y. G. Zeng, S. C. Tian, S. L. Shu, J. Zhang, and L. J. Wang, Appl. Phys. Express **9**, 112102 (2016).
18. M. Winterfeldt, P. Crump, S. Knigge, A. Maaßdorf, U. Zeimer, and G. Erbert, IEEE Photonics Technol. Lett. **27**, 1809 (2015).
19. L. J. Wang, Z. Li, C. Z. Tong, S. L. Shu, S. C. Tian, J. Zhang, X. Zhang, and L. J. Wang, Appl. Opt. **57**, F15 (2018).
20. H. C. Eckstein, U. D. Zeitner, A. Tünnermann, W. Schmid, U. Strauss, and C. Lauer, Opt. Lett. **38**, 4480 (2013).
21. S. Hengesbach, S. Klein, M. Traub, and U. Witte, Opt. Lett. **41**, 595 (2016).
22. Y. F. Zhao, F. Y. Sun, C. Z. Tong, S. L. Shu, G. Y. Hou, H. Y. Lu, X. Zhang, L. J. Wang, S. C. Tian, and L. J. Wang, Opt. Express **26**, 14058 (2018).
23. D. Heydari, Y. Bai, N. Bandyopadhyay, S. Slivken, and M. Razeghi, Appl. Phys. Lett. **106**, 091105 (2015).
24. J. M. Rong, E. B. Xing, Y. Zhang, L. J. Wang, S. L. Shu, S. C. Tian, C. Z. Tong, X. L. Chai, Y. Q. Xu, H. Q. Ni, Z. C. Niu, and L. J. Wang, Opt. Express **24**, 7246 (2016).
25. R. Kaspi, S. Luong, C. Yang, C. Lu, T. C. Newell, and T. Bate, Appl. Phys. Lett. **109**, 211102 (2016).
26. M. J. Miah, S. Strohmaier, G. Urban, and D. Bimberg, Appl. Phys. Lett. **113**, 221107 (2018).
27. P. Crump, P. Leisher, T. Matson, V. Anderson, D. Schulte, J. Bell, J. Farmer, M. DeVito, R. Martinsen, Y. K. Kim, K. D. Choquette, G. Erbert, and G. Tränkle, Appl. Phys. Lett. **92**, 131113 (2008).